2009 American Control Conference
Hyatt Regency Riverfront, St. Louis, MO, USA
June 10-12, 2009

Output-Feedback Adaptive Control of Electrostatic Microactuators

Keng-Peng Tee, Shuzhi Sam Ge and Eng Hock Tay

Abstract— **Adaptive control is presented for a class of electrostatic micro-actuators with bidirectional drive. The objective is to track a reference trajectory within the air gap without knowledge of the plant parameters. Motivated by practical difficulties in measuring velocity of the moving plate, an output feedback scheme is developed. After transforming the plant into the parametric output feedback form, adaptive observer backstepping is employed to achieve asymptotic output tracking. To prevent contact of the movable plate and the electrodes, asymmetric barrier functions are employed in Lyapunov synthesis. All closed loop signals are ensured to be bounded. A simulation study demonstrates the effectiveness of the proposed control.**

I. Introduction

The control of micro-scale devices has gained increasing attention in recent decades, spurred by the advent of microelectromechanical systems (MEMs) technology, which allows for micro-scale devices to be batch-produced and processed at low costs. Among the different types of micro-scale actuators, electrostatic microactuators have gained widespread acceptance in MEMs applications, due to the simplicity of their structure, ease of fabrication, and the favorable scaling of electrostatic forces into the micro domain.

One of the main problems associated with uni-directional electrostatic actuation with open loop voltage control is the pull-in instability, which places a severe limit on the operating range of electrostatic actuators. To overcome this problem, many methods have been proposed, including voltage control with position feedback [1], passive addition of series capacitor [2], [3], charge feedback [4], and nonlinear control techniques [5], [6]. Electrostatic micro-actuators with bidirectional drive [7], [8], [9] are not significantly affected by pull-in due to the fact that they can be actively controlled in both directions. As a result, an extended range of travel is achievable and the added controllability is an advantage in high performance applications. We focus on bidirectional micro-actuators in this paper.

In designing a control for electrostatic micro-actuators, plant model parameters are usually required, and it is common to estimate them through offline system identification methods. However, inconsistencies in bulk micromachining result in variation of parameters across pieces, and may require extensive efforts in parameter identification, with higher costs. Furthermore, some of the parameters, such as the damping constant, are usually difficult to identify accurately, so a viable alternative is to rely on adaptive feedback control for online compensation of parametric uncertainties [10], [11].

In this paper, we extend our previous results [11], which tackled full-state feedback adaptive control of uncertain electrostatic microactuators, to the output feedback case, motivated by the fact that velocity feedback is unavailable in practice. We consider single degree-of-freedom (1DOF) electrostatic microactuators with bidirectional drive, described in Section II, which can be transformed into the parametric output feedback form. Adaptive observer backstepping is then employed to force the movable electrode to track a reference trajectory within the air gap without knowledge of plant parameters or velocity measurements, as shown in Section III. To prevent the movable electrode from coming into contact with the fixed electrodes, we employ asymmetric barrier functions in Lyapunov synthesis, motivated by the approach of tailoring the Lyapunov function according to the requirements of the problem (e.g. [12], [13]). To illustrate the performance of the control, a simulation study is presented in Section IV.

II. Problem Formulation and Preliminaries

Consider the dynamic model of the 1-DOF electrostatic microactuator with bidirectional drive, as illustrated in Figure 1. The state space equations governing the dynamics of the electrostatic microactuator are given by:

$$m\ddot{l} + b\dot{l} + kl = \frac{\epsilon A}{2}\left(\frac{V_f^2}{(l_0 - l)^2} - \frac{V_b^2}{(l_0 + l)^2}\right) =: \frac{\epsilon A}{2}\nu \tag{1}$$

where m denotes the mass of the movable electrode, ϵ the permittivity of the gap, A the plate area, b and k the damping and spring constants respectively, all of which are *uncertain* parameters.

The constant parameters m, ϵ, A, b and k may be difficult to identify accurately in practice, and are thus considered to be uncertain. For example, m, r, and A can vary from unit to unit due to limitations in fabrication precision. The permittivity can change according to the ambient humidity. While stiffness k can be estimated from experimentation and pull-in analysis, the damping constant is typically difficult to obtain due to the fact that it is caused by complex processes such friction and viscous fluid forces [9]. Nevertheless, it is reasonable to have good indication of the order of magnitudes of these parameters.

This work is partially supported by Agency for Science, Technology and Research, Singapore (A*STAR) SERC Grant No. 052-101-0097.

K. P. Tee is with the Institute for Infocomm Research, A*STAR, Singapore 138632 kptee@i2r.a-star.edu.sg

S. S. Ge is with the Department of Electrical & Computer Engineering, National University of Singapore, Singapore 117576 samge@nus.edu.sg

E. H. Tay is with the Department of Mechanical Engineering, National University of Singapore, Singapore 117576 mpetayeh@nus.edu.sg

978-1-4244-4524-0/09/$25.00 ©2009 AACC

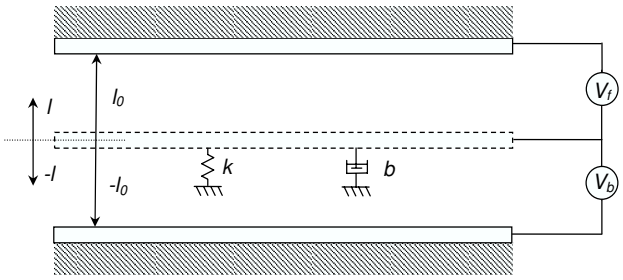

Fig. 1. Single degree-of-freedom electrostatic microactuator with bidirectional drive

Remark 1: In practice, the displacement l can be measured by state-of-the-art capacitive sensing methods. The only difficulty is in the measurement of the velocity $\dot{l}$, thus motivating the importance of output feedback designs.

To obtain the same order of magnitude of the variables and thereby avoid numerical problems in simulation, we perform a change of time scale $\tau = \sigma t$ and change of variables $x_1 = l/l_0$, $x_2 = (1/l_0)(dl/d\tau)$, $u = \nu/\beta$, for large constants $\sigma > 0$ and $\beta > 0$, thus yielding:

$$\begin{aligned} \frac{dx_1}{d\tau} &= x_2(\tau) \\ \frac{dx_2}{d\tau} &= -\frac{b}{m\sigma}x_2(\tau) - \frac{k}{m\sigma^2}x_1(\tau) + \frac{\epsilon A\beta}{2m\sigma^2 l_0}u(\tau) \\ y &= x_1(\tau) \end{aligned} \tag{2}$$

where $y \in R$ is the output. For ease of notation, $\dot{x}_1$ and $\dot{x}_2$ are henceforth understood as $dx_1/d\tau$ and $dx_2/d\tau$ respectively, following the change of time scale.

The control objective is to force the movable electrode to track a reference trajectory $y_d(t)$ within the air gap, i.e. $|y(t) - y_d(t)| \to 0$ as $t \to \infty$. Additionally, the control is required to prevent the movable plate from coming into contact with the electrodes, so as to avoid mechanical wear, impact-related perturbations to performance, and complicated switched systems analysis.

Assumption 1: The first and second order time-derivatives of the reference trajectory $y_d(t)$ are bounded, i.e. $\dot{y}_d < Y_1$, $\ddot{y}_d < Y_2$, where Y_1 and Y_2 are constants. In addition, the reference trajectory is bounded by $\underline{y}_d \le y_d(t) \le \overline{y}_d$, where $\underline{y}_d$ and $\overline{y}_d$ are constants that satisfy $\underline{y}_d > -1 + \frac{\delta}{l_0}$ and $\overline{y}_d < 1 - \frac{\delta}{l_0}$.

To design a control that does not violate the constraint on the output, we employ a barrier function $V_1(z_1)$ (Figure 2b) in Lyapunov synthesis, which satisfies $V_1(z_1) \to \infty$ as $z_1 \to -\sqrt{k_a}$ or $z_1 \to \sqrt{k_b}$.

Lemma 1: For trajectories $z_1(t)$, $z_2(t)$ starting from $z_1(0) \in (-\sqrt{k_a}, \sqrt{k_b})$, $z_2(0) \in \mathbb{R}$, where k_a and k_b are positive constants, if there exists a continuously differentiable and positive definite function

$$V(z_1, z_2) = V_1(z_1) + V_2(z_2)$$

defined on $z_1 \in (-\sqrt{k_a}, \sqrt{k_b})$, $z_2 \in \mathbb{R}$, such that

$$V_1(z_1) \to \infty \text{ as } z_1 \to -\sqrt{k_a} \text{ or } z_1 \to \sqrt{k_b}$$
$$\gamma_1(|z_2|) \le V_2(z_2) \le \gamma_2(|z_2|)$$

with γ_1 and γ_2 as class K_∞ functions, and the following inequality holds:

$$\dot{V} \le 0$$

then $z_1(t)$ remains in the open set $z_1 \in (-\sqrt{k_a}, \sqrt{k_b})$ $\forall t > 0$.

Proof: Since $V(z_1, z_2)$ is positive definite and $\dot{V}(z_1, z_2) \le 0$, it is implied that $V(z_1, z_2)$ is bounded $\forall t > 0$. From $V(z_1, z_2) = V_1(z_1) + V_2(z_2)$ and the fact that $V_1(z_1)$ and $V_2(z_2)$ are positive functions, we can infer that since $V(z_1, z_2)$ is bounded, $V_1(z_1)$ is necessarily bounded as well. Because $V_1(z_1)$ is bounded, we know, from (3), that $z_1 \neq \sqrt{k_b}$ and $z_1 \neq -\sqrt{k_a}$. Given that $-\sqrt{k_a} < z_1(0) < \sqrt{k_b}$, it can be concluded that $-\sqrt{k_a} < z_1(t) < \sqrt{k_b}$, $\forall t > 0$. ■

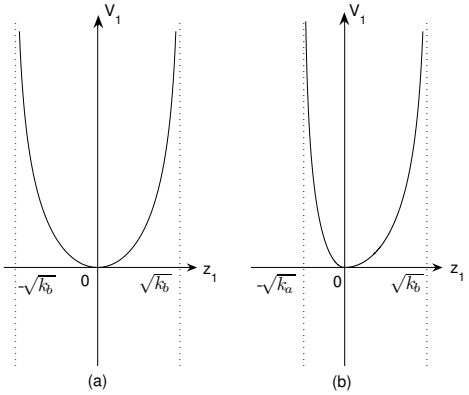

Fig. 2. Schematic illustration of (a) symmetric and (b) asymmetric barrier functions.

III. Adaptive Output Feedback Control Design

To facilitate the design of the adaptive observer backstepping control [14], we first perform a change of coordinates:

$$\begin{aligned} \eta_1 &= x_1 \\ \eta_2 &= x_2 + \frac{b}{m\sigma}x_1 \end{aligned}$$

so as to rewrite the system dynamics (2) into the parametric output feedback form:

$$\begin{aligned} \dot{\eta}_1 &= \eta_2 - \theta_1\eta_1 \\ \dot{\eta}_2 &= -\theta_2\eta_1 + \vartheta u \\ y &= \eta_1 \end{aligned} \tag{3}$$

where

$$\theta_1 = \frac{b}{m\sigma}, \quad \theta_2 = \frac{k}{m\sigma^2}, \quad \vartheta = \frac{\epsilon A\beta}{2m\sigma^2 l_0} \tag{4}$$

This can be represented by the simplified form:

$$\begin{aligned} \dot{\eta} &= A\eta + \sum_{i=1}^{2}\theta_i\phi_i(y) + \vartheta e_2 u \\ y &= \eta_1 \end{aligned} \tag{5}$$

where $e_2 := [0,1]^T$, $\eta = [\eta_1, \eta_2]^T$, $A = \begin{bmatrix} 0 & 1 \\ 0 & 0 \end{bmatrix}$, $\phi_1(y) = [-y, 0]^T$, $\phi_2(y) = [0, -y]^T$.

Design the following filters:

$$\dot{\xi}_0 = A_0\xi_0 + cy \tag{6}$$

$$\dot{\xi}_i = A_0\xi_i + \phi_i(y), \quad i = 1,2 \tag{7}$$

$$\dot{v} = A_0 v + e_2 u + \varphi \tag{8}$$

where $\xi_i \in R^2$ $(i = 0, 1, 2)$, $v \in R^2$, $\varphi(\cdot) = [\varphi_1, \varphi_2]^T \in R^2$ is a correction function to be designed, and $c = [c_1, c_2]^T$ with positive constants c_1 and c_2 chosen such that the matrix $A_0 = \begin{bmatrix} -c_1 & 1 \\ -c_2 & 0 \end{bmatrix}$ satisfies

$$A_0^T P + P A_0 = -R \tag{9}$$

for some $P = P^T > 0$ and $R = R^T > 0$.

By constructing the state estimate as follows

$$\hat{\eta}(t) = \xi_0(t) + \sum_{i=1}^{2} \theta_i \xi_i(t) + \vartheta v(t) \tag{10}$$

it is easy to see that the dynamics of the observation error, $\tilde{\eta} = \hat{\eta} - \eta$, are given by

$$\begin{aligned} \dot{\tilde{\eta}} = \dot{\hat{\eta}} - \dot{\eta} &= A_0\left(\xi_0 + \sum_{i=1}^{2}\theta_i\xi_i + \vartheta v\right) - A_0\eta + \vartheta\varphi \\ &= A_0\tilde{\eta} + \vartheta\varphi \end{aligned} \tag{11}$$

where the correction term $\varphi(\cdot)$ is designed later. The constructive procedure for adaptive observer backstepping design will be presented next.

Step 1: Define $z_1 = y - y_d$, whose derivative is given by

$$\dot{z}_1 = \xi_{02} + \sum_{i=1}^{2}\theta_i\xi_{i2} + \vartheta v_2 - \tilde{\eta}_2 - \theta_1 y - \dot{y}_d \tag{12}$$

where ξ_{ij} and v_j denote the j-th elements of ξ_i and v, respectively. Denote $z_2 = v_2 - \alpha_1$, where α_1 is a virtual control to be designed. Consider the asymmetric barrier Lyapunov function candidate:

$$\begin{aligned} V_1 = &\frac{\kappa_0}{2} q(z_1) \log\frac{k_b}{k_b - z_1^2} + \frac{\kappa_0}{2}(1 - q(z_1)) \log\frac{k_a}{k_a - z_1^2} \\ &+ \frac{1}{2}\tilde{\Theta}_1^T\Gamma_1^{-1}\tilde{\Theta}_1 + \frac{\vartheta}{2\gamma_\varrho}\tilde{\varrho}^2 \end{aligned} \tag{13}$$

where $\kappa_0 > 0$ is a constant, $\Gamma_1 = \Gamma_1^T > 0$ is a constant matrix, $\tilde{\Theta}_1 = \hat{\Theta}_1 - \Theta_1$ and $\tilde{\varrho} = \hat{\varrho} - \varrho$ are the estimation errors for the unknown parameters $\Theta_1 := [\theta_1, \theta_2]^T$ and $\varrho := 1/\vartheta$, respectively, and the function $q(\cdot) : R \to \{0, 1\}$ is given by

$$q(\bullet) = \begin{cases} 1, & \text{if } \bullet > 0 \\ 0, & \text{if } \bullet \le 0 \end{cases} \tag{14}$$

and

$$k_a = \left(1 - \frac{\delta}{l_0} - |\underline{y}_d|\right)^2, \qquad k_b = \left(1 - \frac{\delta}{l_0} - |\overline{y}_d|\right)^2 \tag{15}$$

are positive constants representing the constraints in the z_1 state space, given by $-\sqrt{k_a} < z_1 < \sqrt{k_b}$, induced from the constraints in the x_1 state space, given by $|x_1| < 1 - \frac{\delta}{l_0}$. For clarity of presentation, a schematic illustration of $V_1(z_1)$ is shown in Figure 2b. Throughout this paper, for ease of notation, we abbreviate $q(z_1)$ by q, unless otherwise stated. The derivative of V_1 is given by

$$\begin{aligned} \dot{V}_1 = &\left(\frac{q}{k_b - z_1^2} + \frac{1-q}{k_a - z_1^2}\right)\kappa_0 z_1[\xi_{02} + \vartheta(z_2 + \alpha_1) \\ &+ \Theta_1^T\Psi_1 - \tilde{\eta}_2 - \dot{y}_d] + \tilde{\Theta}_1^T\Gamma_1^{-1}\dot{\hat{\Theta}}_1 + \frac{\vartheta}{\gamma_\varrho}\tilde{\varrho}\dot{\hat{\varrho}} \end{aligned} \tag{16}$$

where $\Psi_1 := [\xi_{12} - y, \xi_{22}]^T$. To facilitate the design of the virtual control and adaptation laws, we express the virtual control in the form

$$\alpha_1 = \hat{\varrho}\bar{\alpha}_1 \tag{17}$$

where

$$\begin{aligned} \bar{\alpha}_1 := &-\xi_{02} - \left[q(k_b - z_1^2) + (1-q)(k_a - z_1^2)\right]\kappa_1 z_1^3 \\ &- \hat{\Theta}_1^T\Psi_1 + \dot{y}_d \end{aligned} \tag{18}$$

Choose the adaptation laws as

$$\dot{\hat{\Theta}}_1 = \Gamma_1\Psi_1\left(\frac{q}{k_b - z_1^2} + \frac{1-q}{k_a - z_1^2}\right)\kappa_0 z_1 \tag{19}$$

$$\dot{\hat{\varrho}} = -\gamma_\varrho\left(\frac{q}{k_b - z_1^2} + \frac{1-q}{k_a - z_1^2}\right)\kappa_0\bar{\alpha}_1 z_1 \tag{20}$$

Substituting (17)-(20) into (16), we obtain

$$\begin{aligned} \dot{V}_1 = &-\kappa_0\kappa_1 z_1^4 + \left(\frac{q}{k_b - z_1^2} + \frac{1-q}{k_a - z_1^2}\right)\kappa_0(\hat{\vartheta} z_1 z_2 \\ &- z_1\tilde{\eta}_2 - \tilde{\vartheta} z_1 z_2) \end{aligned} \tag{21}$$

where $\tilde{\vartheta} = \hat{\vartheta} - \vartheta$. From the above equation, it can be seen that the first term is stabilizing, while the second term consisting of state and parameter estimation errors will be brought forward into the subsequent step to be handled by the actual control.

In the following lemma, we assert that $\alpha_1(z_1, \cdot)$ is a C^1 function, which ensures that $\dot{\alpha}_1$ is well-defined.

Lemma 2: The virtual control $\alpha_1(z_1, \cdot)$ in (17) is continuous and C^1 continuously differentiable with respect to z_1 in the open interval $z_1 \in (-\sqrt{k_a}, \sqrt{k_b})$.

Proof: For $0 < z_1 < \sqrt{k_b}$, we have

$$\alpha_1 = \hat{\varrho}[-\xi_{02} - \hat{\Theta}_1^T\Psi_1 - (k_b - z_1^2)\kappa_1 z_1^3 + \dot{y}_d] \tag{22}$$

and for $-\sqrt{k_a} < z_1 < 0$, we have

$$\alpha_1 = \hat{\varrho}[-\xi_{02} - \hat{\Theta}_1^T\Psi_1 - (k_a - z_1^2)\kappa_1 z_1^3 + \dot{y}_d] \tag{23}$$

It is easy to see that $\lim_{z_1 \to 0^+}\alpha_1 = \lim_{z_1 \to 0^-}\alpha_1 = \hat{\varrho}(-\xi_{02} - \hat{\Theta}_1^T\Psi_1 + \dot{y}_d)$, leading to the fact that α_1 is continuous in $z_1 \in (-\sqrt{k_a}, \sqrt{k_b})$.

The virtual control $\alpha_1(z_1, \cdot)$ is piecewise C^1, with respect to z_1, over the two intervals $z_1 \in (-\sqrt{k_a}, 0]$ and $z_1 \in (0, \sqrt{k_b})$. Thus, to show that α_1 is a C^1 function for $-\sqrt{k_a} < z_1 < \sqrt{k_b}$, we need only to show that $\lim_{z_1 \to 0}\frac{\partial\alpha_1}{\partial z_1}$ is identical from both directions. For $0 < z_1 < \sqrt{k_b}$, we have

$$\lim_{z_1 \to 0^+}\frac{\partial\alpha_1}{\partial z_1} = \lim_{z_1 \to 0^+}\hat{\varrho}\kappa_1\left(-3k_b + 5z_1^2\right)z_1^2 = 0 \tag{24}$$

Similarly, for $-\sqrt{k_a} < z_1 < 0$, we obtain that

$$\lim_{z_1 \to 0^-} \frac{\partial \alpha_1}{\partial z_1} = \lim_{z_1 \to 0^-} \hat{\varrho} \kappa_1 \left(-3k_a + 5z_1^2\right) z_1^2 = 0 \qquad (25)$$

Hence, $\lim_{z_1 \to 0^+} \frac{\partial \alpha_1}{\partial z_1} = \lim_{z_1 \to 0^-} \frac{\partial \alpha_1}{\partial z_1}$, and we conclude that $\alpha_1(z_1, \cdot)$ is C^1 with respect to z_1. ■

Step 2: This is the second and final step of the backstepping procedure, in which the control input u appears. According to Lemma 2, the derivative of the virtual control $\alpha_1(\xi_0, \xi_1, \xi_2, y, \hat{\Theta}_1, \hat{\varrho}, y_d, \dot{y}_d)$ is well-defined, and can be computed as:

$$\begin{aligned}
\dot{\alpha}_1 &= \frac{\partial \alpha_1}{\partial \xi_0}(A_0\xi_0 + cy) + \sum_{i=1}^{2} \frac{\partial \alpha_1}{\partial \xi_i}(A_0\xi_i + \phi_i) \\
&+ \frac{\partial \alpha_1}{\partial z_1}\left(\xi_{02} + \sum_{i=1}^{2} \theta_i \xi_{i2} + \vartheta v_2 - \tilde{\eta}_2 - \theta_1 y - \dot{y}_d\right) \\
&+ \frac{\partial \alpha_1}{\partial \hat{\Theta}_1}\Gamma_1 \Psi_1 \left(\frac{q}{k_b - z_1^2} + \frac{1-q}{k_a - z_1^2}\right) \kappa_0 z_1 \\
&- \frac{\partial \alpha_1}{\partial \hat{\varrho}} \gamma_\varrho \left(\frac{q}{k_b - z_1^2} + \frac{1-q}{k_a - z_1^2}\right) \kappa_0 \bar{\alpha}_1 z_1 \\
&+ \sum_{i=0}^{1} \frac{\partial \alpha_1}{\partial y_d^{(i)}} y_d^{(i+1)} \qquad (26)
\end{aligned}$$

where $y_d^{(i)} := \frac{d^i}{dt^i}(y_d)$, and the partial derivatives are obtained as:

$$\begin{array}{lll}
\frac{\partial \alpha_1}{\partial \xi_0} = -e_2^T \hat{\varrho}, & \frac{\partial \alpha_1}{\partial \xi_1} = -e_2^T \hat{\varrho} \hat{\Theta}_{11}, & \frac{\partial \alpha_1}{\partial \xi_2} = -e_2^T \hat{\varrho} \hat{\Theta}_{12}, \\
\frac{\partial \alpha_1}{\partial y} = \hat{\varrho} & \frac{\partial \alpha_1}{\partial \hat{\Theta}_1} = -\hat{\varrho} \Psi_1^T, & \frac{\partial \alpha_1}{\partial \hat{\varrho}} = \bar{\alpha}_1, \\
\frac{\partial \alpha_1}{\partial y_d} = \hat{\varrho} \hat{\Theta}_{11}, & & \\
\frac{\partial \alpha_1}{\partial z_1} = \hat{\varrho}\left[\hat{\Theta}_{11} - 3\left(qk_b + (1-q)k_a\right)\kappa_1 z_1^2 + 5\kappa_1 z_1^4\right] & &
\end{array}$$

with Θ_{1i} denoting the i-th element of Θ_1, for $i = 1, 2$. From Lemma 2, we deduce that $\dot{\alpha}_1$ is continuous. Note that (26) can be written as the sum of two parts $F(\cdot)$ and $G(\cdot)$:

$$\dot{\alpha}_1 = F\left(\xi_0, \xi_1, \xi_2, z_1, \hat{\Theta}_1, \hat{\varrho}, y_d, \dot{y}_d\right) + G\left(\theta_1, \theta_2, \vartheta, \tilde{\eta}\right) \quad (27)$$

in which $F(\cdot)$ is known and can be directly cancelled by the control u, while $G(\cdot)$ contains unknown elements. The functions $F(\cdot)$ and $G(\cdot)$ are defined as follows

$$\begin{aligned}
F &= \frac{\partial \alpha_1}{\partial \xi_0}(A_0\xi_0 + cy) + \sum_{i=1}^{2} \frac{\partial \alpha_1}{\partial \xi_i}(A_0\xi_i + \phi_i) \\
&+ \frac{\partial \alpha_1}{\partial \hat{\Theta}_1}\Gamma_1 \Psi_1 \left(\frac{q}{k_b - z_1^2} + \frac{1-q}{k_a - z_1^2}\right) \kappa_0 z_1 \\
&- \frac{\partial \alpha_1}{\partial \hat{\varrho}} \gamma_\varrho \left(\frac{q}{k_b - z_1^2} + \frac{1-q}{k_a - z_1^2}\right) \kappa_0 \bar{\alpha}_1 z_1 \\
&+ \frac{\partial \alpha_1}{\partial z_1}(\xi_{02} - \dot{y}_d) + \sum_{i=0}^{1} \frac{\partial \alpha_1}{\partial y_d^{(i)}} y_d^{(i+1)} \\
&= \hat{\varrho}\omega - \gamma_\varrho \left(\frac{q}{k_b - z_1^2} + \frac{1-q}{k_a - z_1^2}\right) \kappa_0 \bar{\alpha}_1^2 z_1 \qquad (28)
\end{aligned}$$

$$\begin{aligned}
G &= \frac{\partial \alpha_1}{\partial z_1}\left(\sum_{i=1}^{2} \theta_i \xi_{i2} + \vartheta v_2 - \tilde{\eta}_2 - \theta_1 y\right) \\
&= \frac{\partial \alpha_1}{\partial z_1}(\Theta_2^T \Psi_2 - \tilde{\eta}_2) \qquad (29)
\end{aligned}$$

where $\Theta_2 = [\theta_1, \theta_2, \vartheta]^T$, $\Psi_2 = [\xi_{12} - y, \xi_{22}, v_2]^T$, $\Psi_{1,a} = [c_2\xi_{11} + \xi_{02}, c_2\xi_{21} + y]^T$ and

$$\begin{aligned}
\omega &= c_2(\xi_{01} - y) + \ddot{y}_d + \hat{\Theta}_1^T \Psi_{1,a} \\
&- \Psi_1^T \Gamma_1 \Psi_1 \left(\frac{q}{k_b - z_1^2} + \frac{1-q}{k_a - z_1^2}\right) \kappa_0 z_1 \qquad (30) \\
&+ \left[-3(qk_b + (1-q)k_a)\kappa_1 z_1^2 + 5\kappa_1 z_1^4\right](\xi_{02} - \dot{y}_d)
\end{aligned}$$

This yields the derivative of z_2 as

$$\dot{z}_2 = -c_2 v_1 + u + \varphi_2 - F(\cdot) - G(\cdot) \qquad (31)$$

Consider the Lyapunov function candidate V_2 as follows:

$$V_2 = V_1 + \frac{1}{2}z_2^2 + \frac{1}{2\vartheta}\tilde{\eta}^T P \tilde{\eta} + \frac{1}{2\gamma_\vartheta}\tilde{\vartheta}^2 + \frac{1}{2}\tilde{\Theta}_2^T \Gamma_2^{-1} \tilde{\Theta}_2 \quad (32)$$

where $\gamma_\vartheta > 0$ is a constant, $\Gamma_2 = \Gamma_2^T > 0$ is a constant matrix, $P > 0$ is a matrix satisfying (9), $\tilde{\Theta}_2 = \hat{\Theta}_2 - \Theta_2$ is the estimation error for the unknown parameter vector $\Theta_2 = [\theta_1, \theta_2, \vartheta]^T$, and $\tilde{\eta} = \hat{\eta} - \eta$ is the observation error. With the help of (9), the derivative of V_2 along (31) is given by

$$\begin{aligned}
\dot{V}_2 &= -\kappa_0\kappa_1 z_1^4 - \frac{1}{2\vartheta}\tilde{\eta}^T R \tilde{\eta} + \left(\frac{q}{k_b - z_1^2} + \frac{1-q}{k_a - z_1^2}\right) \\
&\times \kappa_0(\hat{\vartheta} z_1 z_2 - z_1 \tilde{\eta}_2) + \tilde{\eta}^T P \varphi + \tilde{\Theta}_2^T \Gamma_2^{-1} \dot{\hat{\Theta}}_2 \\
&+ \tilde{\vartheta}\left[-\left(\frac{q}{k_b - z_1^2} + \frac{1-q}{k_a - z_1^2}\right)\kappa_0 z_1 z_2 + \frac{1}{\gamma_\vartheta}\dot{\hat{\vartheta}}\right] \\
&+ z_2[-c_2 v_1 + u + \varphi_2 - F(\cdot) + \hat{\varrho}[\hat{\Theta}_{11} - 3(qk_b \\
&+ (1-q)k_a)\kappa_1 z_1^2 + 5\kappa_1 z_1^4](-\Theta_2^T \Psi_2 + \tilde{\eta}_2)] \qquad (33)
\end{aligned}$$

Design the correction term φ as:

$$\begin{aligned}
\varphi &= -\left[\hat{\varrho}[\hat{\Theta}_{11} - 3\left(qk_b + (1-q)k_a\right)\kappa_1 z_1^2 + 5\kappa_1 z_1^4] z_2 \right. \\
&\left. - \left(\frac{q}{k_b - z_1^2} + \frac{1-q}{k_a - z_1^2}\right)\kappa_0 z_1\right] P^{-1} e_2 \qquad (34)
\end{aligned}$$

and the control and adaptation laws as:

$$\begin{aligned}
u &= -\kappa_2 z_2 + c_2 v_1 - \hat{\vartheta}\left(\frac{q}{k_b - z_1^2} + \frac{1-q}{k_a - z_1^2}\right)\kappa_0 z_1 \\
&+ \frac{\partial \alpha_1}{\partial z_1}\hat{\Theta}_2^T \Psi_2 + F(\cdot) - \varphi_2 \qquad (35) \\
\dot{\hat{\Theta}}_2 &= -\frac{\partial \alpha_1}{\partial z_1}\Gamma_2 \Psi_2 z_2 \qquad (36) \\
\dot{\hat{\vartheta}} &= \gamma_\vartheta\left(\frac{q}{k_b - z_1^2} + \frac{1-q}{k_a - z_1^2}\right)\kappa_0 z_1 z_2 \qquad (37)
\end{aligned}$$

Substituting (35)-(37) into (33), we arrive at

$$\dot{V}_2 = -\kappa_0\kappa_1 z_1^4 - \kappa_2 z_2^2 - \frac{1}{2\vartheta}\tilde{\eta}^T R \tilde{\eta} \qquad (38)$$

in which all three terms on the right hand side are always non-positive.

Since u is an aggregate control variable defined for ease of analysis, we still need to compute the actual voltage controls

V_f and V_b according to (1), which is performed with the following algorithm

$$\begin{aligned} V_f &= \sqrt{\beta l_0^2 q(u)(1-x_1)^2 u} \\ V_b &= \sqrt{-\beta l_0^2 (1-q(u))(1+x_1)^2 u} \end{aligned} \tag{39}$$

where the function $q(\cdot)$ is defined in (14). It can be checked that $\beta l_0^2 q(u)(1-x_1)^2 u$ and $-\beta l_0^2(1-q(u))(1+x_1)^2 u$, i.e., the terms within the square root operators, are always non-negative.

Remark 2: It can be checked that the control $u = u(y, v, \xi_0, \xi_1, \xi_2, \hat{\Theta}_1, \hat{\Theta}_2, \hat{\varrho}, \hat{\vartheta}, y_d, \dot{y}_d, \ddot{y}_d)$, where the filter signals $\xi_0(t), \xi_1(t), \xi_2(t)$ are generated from $y(t)$, the signal $v(t)$ from $u(t)$, the parameter estimates $\hat{\Theta}_1, \hat{\Theta}_2, \hat{\varrho}, \hat{\vartheta}$ from $y, y_d, \dot{y}_d, \xi_0, \xi_1, \xi_2$. Therefore, the control u is feasible based on only output measurement, and does not require the feedback of the state x_2.

Theorem 1: Consider the uncertain 1DOF electrostatic microactuator system (2) under Assumption 1, output feedback control law (35), and adaptation laws (19), (20), (36), and (37). For initial conditions satisfying $x(0) \in \bar{\Omega}$ where

$$\bar{\Omega} := \{x \in R^2 \mid y_d(0) - \sqrt{k_a} < x_1 < y_d(0) + \sqrt{k_b}\}$$

the output tracking error with respect to any reference trajectory within the air gap, i.e.

$$y_d(t) \in (-l_0 + \delta, l_0 - \delta)$$

is asymptotically stabilized, i.e., $y(t) \to y_d(t)$ as $t \to \infty$, and all closed loop signals remain bounded. Furthermore, the output $y(t)$ remains in the set

$$\Omega_y := \{y \in \mathbb{R} \ : \ |y| < 1 - \delta/l_0\}$$

$\forall t > 0$, i.e. the output constraint is never violated.

Proof: First, we show that all closed loop signals are bounded. From (38), we know that $\dot{V}_2(t) \leq 0 \ \forall t > 0$, and thus, the error signals $z_1(t)$, $z_2(t)$, $\tilde{\Theta}_1(t)$, $\tilde{\Theta}_2(t)$, $\tilde{\varrho}(t)$, $\tilde{\vartheta}(t)$, and $\tilde{\eta}(t)$ are bounded. Since Θ_1, Θ_2, ϱ, ϑ are constants, we have that $\hat{\Theta}_1(t)$, $\hat{\Theta}_2(t)$, $\hat{\varrho}(t)$, $\hat{\vartheta}(t)$ are bounded. The boundedness of $z_1(t)$ and the reference trajectory $y_d(t)$ implies boundedness of the output $y(t)$. From the filters (6)-(7), we know that $\xi_i(t)$ $(i = 0, 1, 2)$ are all bounded.

Given that $\dot{y}_d(t)$ is bounded, the virtual control α_1 is also bounded from (17). This leads to the boundedness of $v_2(t) = z_2(t) + \alpha_1(t)$, and $\varphi(t)$, which implies that $v_1(t)$ is bounded. According to Lemma 1, the tracking error $z_1(t)$ remains in the set $-\sqrt{k_a} < z_1 < \sqrt{k_b} \ \forall t > 0$. Thus, we can deduce that the control $u(t)$ in (35), as well as the adaptation rates $\dot{\hat{\Theta}}_1$, $\dot{\hat{\varrho}}$, $\dot{\hat{\Theta}}_2$, $\dot{\hat{\vartheta}}$ in (19), (20), (36), (37) respectively, are all bounded. At the same time, from (10), it follows that $\hat{\eta}(t)$ is bounded, which in turn implies that $\eta_2(t)$, and thus $x_2(t)$, are bounded. Therefore, all closed loop signals are bounded.

Next, we prove that $y(t) \to y_d(t)$ as $t \to \infty$. From

$$\ddot{V}_2 = -4\kappa_1 z_1^3 \dot{z}_1 - 2\kappa_2 z_2 \dot{z}_2 - 2\tilde{\eta}^T R \dot{\tilde{\eta}}$$

we know that $\ddot{V}_2(t)$ is bounded, since $\dot{z}_1$ is bounded from (12), $\dot{z}_2$ is bounded from (31), and $\dot{\tilde{\eta}}$ is bounded from (11). Hence, $\dot{V}(t)$ is uniformly continuous. According to Barbalat's Lemma, $z_1(t), z_2(t) \to 0$ as $t \to \infty$. Since $z_1(t) = x_1(t) - y_d(t)$, it is clear that $y(t) \to y_d(t)$ as $t \to \infty$.

Lastly, to show that $y \in \Omega_y$, note that $\dot{V}_2(t) \leq 0 \ \forall t > 0$, which implies that for any bounded $V_2(0)$, we have that $V_2(t)$ remains bounded $\forall t > 0$. From (32), it follows that $V_1(t)$ is also bounded $\forall t > 0$, and thus, $-\sqrt{k_a} < z_1 < \sqrt{k_b}$ from Lemma 1. From (15) and $z_1 = y - y_d$, it can be shown that

$$-1 + \frac{\delta}{l_0} + y_d + |\underline{y}_d| < \quad y \quad < 1 - \frac{\delta}{l_0} + y_d - |\overline{y}_d|$$

From Assumption 1, we know that $\underline{y}_d \leq y_d \leq \overline{y}_d$, which yields fact that $y_d + |\underline{y}_d| \geq 0$ and $y_d - |\overline{y}_d| \leq 0$, leading to the following inequality

$$-1 + \frac{\delta}{l_0} < \quad y \quad < 1 - \frac{\delta}{l_0}$$

Hence, we can conclude that $y(t) \in \Omega_y \ \forall t > 0$. ■

IV. Simulation Results

To demonstrate the effectiveness of the control design, we perform simulation for (2) with parameter values: $b = 5.5 \times 10^{-3} N s m^{-1}$, $k = 350.0 N m^{-1}$, $m = 7.32 \times 10^{-10} kg$, $\epsilon = 8.859 \times 10^{-12} F m^{-1}$, $A = 7.854 \times 10^{-7} m^2$, $l_0 = 1.5 \times 10^{-6} m$, $\delta = 3.0 \times 10^{-8} m$. The scaling constants are $\sigma = 1.0 \times 10^6$, $\beta = 1.0 \times 10^{16}$, and the initial conditions $x_1(0) = 0.0$, $x_2(0) = 0.0$, $\hat{\theta}_1(0) = 0.0$, and $\hat{\theta}_2(0) = 0.0$.

The performance of the proposed control, given by (35)-(37) and (39), is investigated for the task of regulating the movable plate at the specified set points y_{si}, $i = 1, 2, 3, 4$. Between the start position and each set point, the plate is to follow a reference trajectory $y_{di}(t)$ defined by:

$$y_{di}(t) = \begin{cases} y_0 + (y_{si} - y_0) d(t) & \text{for } t \leq t_{di} \\ y_{si} & \text{for } t > t_{di} \end{cases} \tag{40}$$

where y_0 is the desired initial position, t_d is the time to reach y_s, starting from y_0, and

$$d(t) = 6(\frac{t}{t_{di}})^5 - 15(\frac{t}{t_{di}})^4 + 10(\frac{t}{t_{di}})^3 \tag{41}$$

We simulate stabilization to four set points within the gap, namely $y_{s1} = -0.2$, $y_{s2} = 0.4$, $y_{s3} = -0.6$, and $y_{s4} = 0.8$, with each case starting from $y_0 = 0.0$. To generate the reference trajectory (40) for each case, we specify the corresponding durations $t_{di} = 50|y_0 - y_{si}| \ \mu s$. The bounds on z_1 corresponding to the set points can be computed as $\sqrt{k_{a1}} = 0.78$, $\sqrt{k_{b1}} = 0.98$, $\sqrt{k_{a2}} = 0.98$, $\sqrt{k_{b2}} = 0.58$, $\sqrt{k_{a3}} = 0.38$, $\sqrt{k_{b3}} = 0.98$, $\sqrt{k_{a4}} = 0.98$, and $\sqrt{k_{b4}} = 0.18$.

For the task of set point regulation, the control parameters are chosen as $\kappa_0 = 1.0$, $\kappa_1 = \kappa_2 = 2.0$, $\Gamma_1 = \text{diag}\{100.0, 500.0\}$, $\Gamma_2 = 100.0 I$, $\gamma_\varrho = 1.0$, $\gamma_\vartheta = 1.0$, $c_1 = 8.0$, $c_2 = 15.0$, $R = I$, and the results are shown in Figures 3-5. From Figure 3, it can be seen that the movable electrode is successfully stabilized at each of the four set points without coming into contact with the electrodes. The boundedness of the control voltages, the velocity and

parameter estimates are shown in Figures 4 and 5. Similar results of asymptotic tracking performance and boundedness of signals are also obtained for the task of tracking a time-varying desired trajectory, but they are omitted due to space constraint.

V. Conclusions

We have presented adaptive output feedback control for a class of 1DOF electrostatic microactuator systems, such that the movable plate is able to track asymptotically a reference trajectory within the air gap without knowledge of the plant parameters, and without any contact between the movable plate and the electrodes. The control design is based on the use of asymmetric barrier functions combined with adaptive observer backstepping. Simulation results show that the proposed adaptive control is effective.

References

[1] P. B. Chu and S. J. Pister, "Analysis of closed-loop control of parallel-plate electrostatic microgrippers," in *Proc. IEEE International Conf. Robotics & Automation*, (San Diego, California), pp. 820–825, May 1994.

[2] J. Seeger and S. Crary, "Stabilization of electrostatically actuated mechanical devices," in *Proc. 9th International Conf. Solid-State Sensors & Actuators (Transducers'97)*, (Chicago, IL), pp. 1133–1136, June 1997.

[3] E. K. Chan and R. W. Dutton, "Electrostatic micromechanical actuator with extended range of travel," *Journal of Microelectromechanical Systems*, vol. 9, no. 3, pp. 321–328, 2000.

[4] R. Nadal-Guardia, A. Deh, R. Aigner, and L. M. Castaer, "Current drive methods to extend the range of travel of electrostatic microactuators beyond the voltage pull-in point," *Journal of Microelectromechanical Systems*, vol. 11, no. 3, pp. 255–263, 2002.

[5] G. Zhu, J. Lévine, and L. Praly, "Improving the performance of an electrostatically actuated MEMs by nonlinear control: Some advances and comparisons," in *Proc. 44th IEEE Conf. Decision & Control*, (Seville, Spain), pp. 7534–7539, December 2005.

[6] D. H. S. Maithripala, J. M. Berg, and W. P. Dayawansa, "Control of an electrostatic microelectromechanical system using static and dynamic output feedback," *Journal of Dynamic Systems, Measurment, and Control*, vol. 127, pp. 443–450, 2005.

[7] K. Nonaka, T. Sugimoto, J. Baillieul, and M. Horenstein, "Bi-directional extension of the travel range of electrostatic actuators by open loop periodically switched oscillatory control," in *Proc. 43rd IEEE Conf. Decision & Control*, (Bahamas), pp. 1964–1969, December 2004.

[8] T. Sugimoto, K. Nonaka, and M. N. Horenstein, "Bidirectional electrostatic actuator operated with charge control," *Journal of Microelectromechanical Systems*, vol. 14, no. 4, pp. 718–724, 2005.

[9] B. Borovic, A. Q. Liu, D. Popa, H. Cai, and F. L. Lewis, "Open-loop versus closed-loop control of MEMs devices: Choices and issues," *Journal of Micromechanics & Microengineering*, vol. 15, pp. 1917–1924, 2005.

[10] D. Piyabongkarn, Y. Sun, R. Rajamani, A. Sezen, and B. J. Nelson, "Travel range extension of a MEMs electrostatic microactuator," *IEEE Trans. Control Systems Technology*, vol. 13, no. 1, pp. 138–145, 2005.

[11] K. P. Tee, S. S. Ge, and E. H. Tay, "Adaptive control of a class of uncertain electrostatic microactuators," in *Proceedings of the American Control Conference*, (New York City, USA), pp. 3186–3191, July 2007.

[12] S. S. Ge, C. C. Hang, and T. Zhang, "A direct adaptive controller for dynamic systems with a class of nonlinear parameterizations," *Automatica*, vol. 35, pp. 741–747, 1999.

[13] K. P. Tee, S. S. Ge, and E. H. Tay, "Barrier Lyapunov Functions for the control of output-constrained nonlinear systems," *Automatica*, 2009, doi: 10.1016/ j.automatica.2008.11.017.

[14] M. Krstic, I. Kanellakopoulos, and P. V. Kokotovic, *Nonlinear and Adaptive Control Design*. New York: Wiley and Sons, 1995.

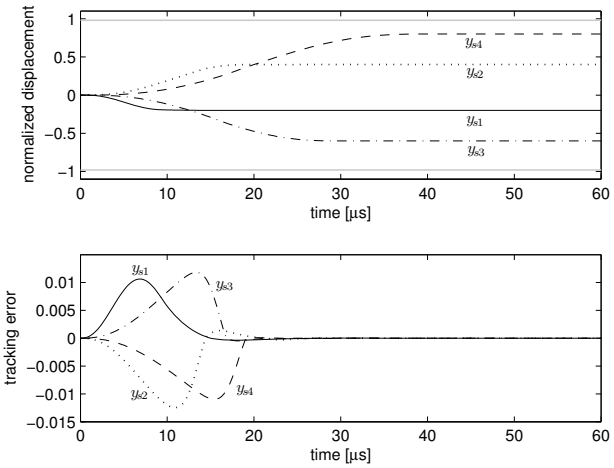

Fig. 3. Normalized displacement x_1 and tracking error z_1

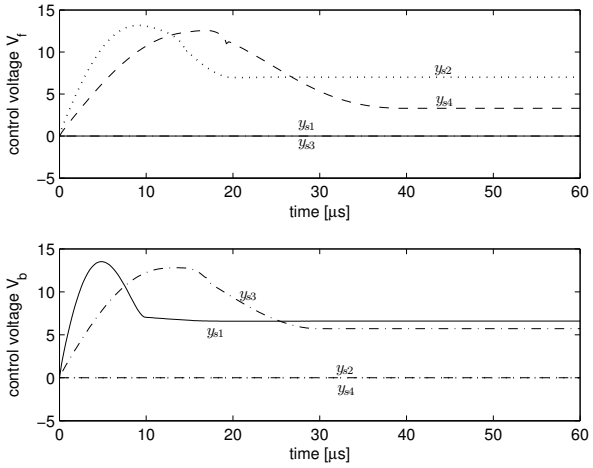

Fig. 4. Control inputs V_f and V_b

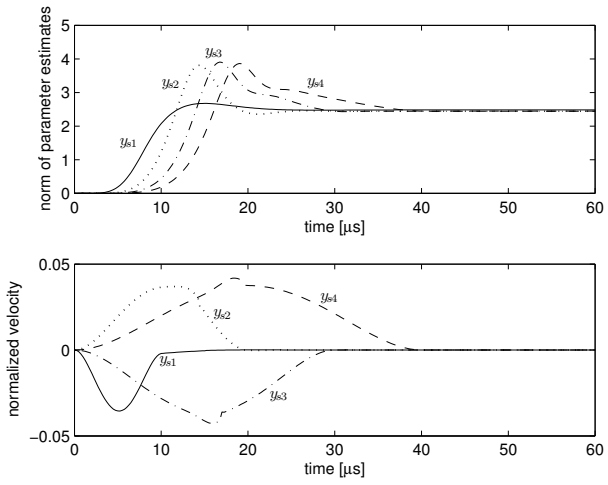

Fig. 5. Norm of parameter estimates and normalized velocity x_2